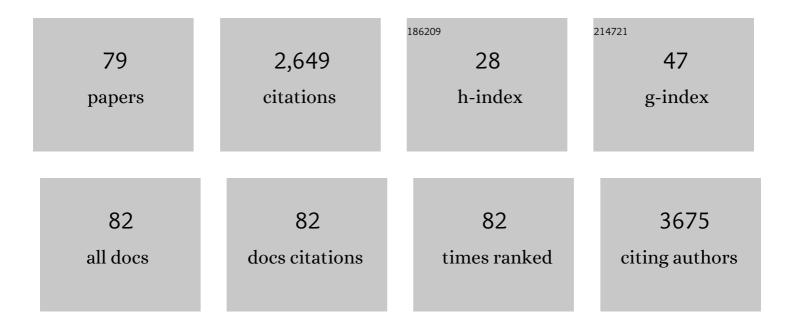
Naoyuki Miyazaki

List of Publications by Year in descending order

Source: https://exaly.com/author-pdf/4732218/publications.pdf Version: 2024-02-01



#	Article	IF	CITATIONS
1	Biological and immunological characteristics of hepatitis E virus-like particles based on the crystal structure. Proceedings of the National Academy of Sciences of the United States of America, 2009, 106, 12986-12991.	3.3	214
2	The Atomic Structure of Rice dwarf Virus Reveals the Self-Assembly Mechanism of Component Proteins. Structure, 2003, 11, 1227-1238.	1.6	144
3	Structure of Hepatitis E Virion-sized Particle Reveals an RNA-dependent Viral Assembly Pathway*. Journal of Biological Chemistry, 2010, 285, 33175-33183.	1.6	140
4	Structure of the green algal photosystem I supercomplex with a decameric light-harvesting complex I. Nature Plants, 2019, 5, 626-636.	4.7	131
5	An ultra-stable gold-coordinated protein cage displaying reversible assembly. Nature, 2019, 569, 438-442.	13.7	124
6	The Crystal Structure of a Virus-like Particle from the Hyperthermophilic Archaeon Pyrococcus furiosus Provides Insight into the Evolution of Viruses. Journal of Molecular Biology, 2007, 368, 1469-1483.	2.0	115
7	Structural basis for energy harvesting and dissipation in a diatom PSII–FCPII supercomplex. Nature Plants, 2019, 5, 890-901.	4.7	92
8	Three-dimensional architecture of podocytes revealed by block-face scanning electron microscopy. Scientific Reports, 2015, 5, 8993.	1.6	77
9	Structures of the wild-type MexAB–OprM tripartite pump reveal its complex formation and drug efflux mechanism. Nature Communications, 2019, 10, 1520.	5.8	77
10	Structural basis for the adaptation and function of chlorophyll f in photosystem I. Nature Communications, 2020, 11, 238.	5.8	75
11	Structural basis for assembly and function of a diatom photosystem I-light-harvesting supercomplex. Nature Communications, 2020, 11, 2481.	5.8	56
12	Giant cadherins Fat and Dachsous self-bend to organize properly spaced intercellular junctions. Proceedings of the National Academy of Sciences of the United States of America, 2014, 111, 16011-16016.	3.3	53
13	Conformational Freedom of the LRP6 Ectodomain Is Regulated by N-glycosylation and the Binding of the Wnt Antagonist Dkk1. Cell Reports, 2017, 18, 32-40.	2.9	51
14	Higher-Order Architecture of Cell Adhesion Mediated by Polymorphic Synaptic Adhesion Molecules Neurexin and Neuroligin. Cell Reports, 2012, 2, 101-110.	2.9	50
15	Structure of a cyanobacterial photosystem I tetramer revealed by cryo-electron microscopy. Nature Communications, 2019, 10, 4929.	5.8	50
16	Association of Rice Gall Dwarf Virus with Microtubules Is Necessary for Viral Release from Cultured Insect Vector Cells. Journal of Virology, 2009, 83, 10830-10835.	1.5	47
17	Arl6IP1 has the ability to shape the mammalian ER membrane in a reticulon-like fashion. Biochemical Journal, 2014, 458, 69-79.	1.7	47
18	Structural variability and complexity of the giant Pithovirus sibericum particle revealed by high-voltage electron cryo-tomography and energy-filtered electron cryo-microscopy. Scientific Reports, 2017, 7, 13291.	1.6	47

Ναογμκι Μιγαζακι

#	Article	IF	CITATIONS
19	Crystal Structure of the cis-Dimer of Nectin-1. Journal of Biological Chemistry, 2011, 286, 12659-12669.	1.6	45
20	High-resolution cryo-EM structure of photosystem II reveals damage from high-dose electron beams. Communications Biology, 2021, 4, 382.	2.0	45
21	Gold Nanoparticle-Induced Formation of Artificial Protein Capsids. Nano Letters, 2012, 12, 2056-2059.	4.5	42
22	Structural visualization of key steps in nucleosome reorganization by human FACT. Scientific Reports, 2019, 9, 10183.	1.6	42
23	Morphological process of podocyte development revealed by block-face scanning electron microscopy. Journal of Cell Science, 2016, 130, 132-142.	1.2	41
24	Structural mechanism of laminin recognition by integrin. Nature Communications, 2021, 12, 4012.	5.8	41
25	Structure and Assembly of a T =1 Virus-Like Particle in BK Polyomavirus. Journal of Virology, 2005, 79, 5337-5345.	1.5	40
26	Transcapsidation and the Conserved Interactions of Two Major Structural Proteins of a Pair of Phytoreoviruses Confirm the Mechanism of Assembly of the Outer Capsid Layer. Journal of Molecular Biology, 2005, 345, 229-237.	2.0	37
27	Tomosyn Inhibits Synaptotagmin-1-mediated Step of Ca2+-dependent Neurotransmitter Release through Its N-terminal WD40 Repeats. Journal of Biological Chemistry, 2010, 285, 40943-40955.	1.6	37
28	Cryo-EM structure of a Marseilleviridae virus particle reveals a large internal microassembly. Virology, 2018, 516, 239-245.	1.1	37
29	Structural Evolution of <i>Reoviridae</i> Revealed by <i>Oryzavirus</i> in Acquiring the Second Capsid Shell. Journal of Virology, 2008, 82, 11344-11353.	1.5	35
30	Dynamic rotation of the protruding domain enhances the infectivity of norovirus. PLoS Pathogens, 2020, 16, e1008619.	2.1	33
31	Phagocytosis is mediated by two-dimensional assemblies of the F-BAR protein GAS7. Nature Communications, 2019, 10, 4763.	5.8	31
32	Structure of a cyanobacterial photosystem I surrounded by octadecameric IsiA antenna proteins. Communications Biology, 2020, 3, 232.	2.0	30
33	Systematic survey of conformational states in β1 and β4 integrins by negative-stain electron microscopy. Journal of Cell Science, 2018, 131, .	1.2	26
34	Megabirnavirus structure reveals a putative 120-subunit capsid formed by asymmetrical dimers with distinctive large protrusions. Journal of General Virology, 2015, 96, 2435-2441.	1.3	24
35	Three-dimensional analysis of morphological changes in the malaria parasite infected red blood cell by serial block-face scanning electron microscopy. Journal of Structural Biology, 2016, 193, 162-171.	1.3	23
36	The Cellular and Mechanical Basis for Response Characteristics of Identified Primary Afferents in the Rat Vibrissal System. Current Biology, 2020, 30, 815-826.e5.	1.8	23

Ναογμκι Μιγαζακι

#	Article	IF	CITATIONS
37	The Amino-Terminal Region of Major Capsid Protein P3 Is Essential for Self-Assembly of Single-Shelled Core-Like Particles of Rice Dwarf Virus. Journal of Virology, 2004, 78, 3145-3148.	1.5	22
38	Serial block-face scanning electron microscopy for three-dimensional analysis of morphological changes in mitochondria regulated by Cdc48p/p97 ATPase. Journal of Structural Biology, 2014, 187, 187-193.	1.3	22
39	ICTV Virus Taxonomy Profile: Megabirnaviridae. Journal of General Virology, 2019, 100, 1269-1270.	1.3	22
40	Viroplasm matrix protein Pns9 from rice gall dwarf virus forms an octameric cylindrical structure. Journal of General Virology, 2011, 92, 2214-2221.	1.3	21
41	Immature morphological properties in subcellular-scale structures in the dentate gyrus of Schnurri-2 knockout mice: a model for schizophrenia and intellectual disability. Molecular Brain, 2017, 10, 60.	1.3	21
42	Three-Dimensional Analysis of the Association of Viral Particles with Mitochondria during the Replication of Rice Gall Dwarf Virus. Journal of Molecular Biology, 2011, 410, 436-446.	2.0	19
43	The infectious particle of insect-borne totivirus-like Omono River virus has raised ridges and lacks fibre complexes. Scientific Reports, 2016, 6, 33170.	1.6	19
44	Putative Neural Network Within an Olfactory Sensory Unit for Nestmate and Non-nestmate Discrimination in the Japanese Carpenter Ant: The Ultra-structures and Mathematical Simulation. Frontiers in Cellular Neuroscience, 2018, 12, 310.	1.8	19
45	Crystallization and preliminary X-ray diffraction analysis of recombinant hepatitis E virus-like particle. Acta Crystallographica Section F: Structural Biology Communications, 2008, 64, 318-322.	0.7	18
46	Structural basis for different types of hetero-tetrameric light-harvesting complexes in a diatom PSII-FCPII supercomplex. Nature Communications, 2022, 13, 1764.	5.8	17
47	The functional organization of the internal components of Rice dwarf virus. Journal of Biochemistry, 2010, 147, 843-850.	0.9	16
48	Life cycle of phytoreoviruses visualized by electron microscopy and tomography. Frontiers in Microbiology, 2013, 4, 306.	1.5	16
49	Mesoscale morphology at nanoscale resolution: serial block-face scanning electron microscopy reveals fine 3D detail of a novel silk spinneret system in a tube-building tanaid crustacean. Frontiers in Zoology, 2016, 13, 14.	0.9	16
50	Physical association between a novel plasma-membrane structure and centrosome orients cell division. ELife, 2016, 5, .	2.8	16
51	Antigenic and Cryo-Electron Microscopy Structure Analysis of a Chimeric Sapovirus Capsid. Journal of Virology, 2016, 90, 2664-2675.	1.5	15
52	Multiple roles of afadin in the ultrastructural morphogenesis of mouse hippocampal mossy fiber synapses. Journal of Comparative Neurology, 2017, 525, 2719-2734.	0.9	14
53	Trpm7 Protein Contributes to Intercellular Junction Formation in Mouse Urothelium. Journal of Biological Chemistry, 2015, 290, 29882-29892.	1.6	12
54	The atomic structures of shrimp nodaviruses reveal new dimeric spike structures and particle polymorphism. Communications Biology, 2019, 2, 72.	2.0	12

Ναογμκι Μιγαζακι

#	Article	IF	CITATIONS
55	Acquired Functional Capsid Structures in Metazoan Totivirus-like dsRNA Virus. Structure, 2020, 28, 888-896.e3.	1.6	12
56	Electron microscopic imaging revealed the flexible filamentous structure of the cell attachment protein P2 ofRice dwarf viruslocated around the icosahedral 5-fold axes. Journal of Biochemistry, 2016, 159, 181-190.	0.9	11
57	Structure of a tetrameric photosystem I from a glaucophyte alga Cyanophora paradoxa. Nature Communications, 2022, 13, 1679.	5.8	11
58	Pleomorphic Configuration of the Trimeric Capsid Proteins of Rice dwarf virus that Allows Formation of Both the Outer Capsid and Tubular Crystals. Journal of Molecular Biology, 2008, 383, 252-265.	2.0	10
59	Zernike phase contrast cryo-electron microscopy reveals 100 kDa component in a protein complex. Journal Physics D: Applied Physics, 2013, 46, 494008.	1.3	8
60	Two conformations of DNA polymerase D-PCNA-DNA, an archaeal replisome complex, revealed by cryo-electron microscopy. BMC Biology, 2020, 18, 152.	1.7	8
61	Atomic Structure of the Human Sapovirus Capsid Reveals a Unique Capsid Protein Conformation in Caliciviruses. Journal of Virology, 2022, 96, e0029822.	1.5	7
62	Ab initiocrystal structure determination of spherical viruses that exhibit a centrosymmetric location in the unit cell. Acta Crystallographica Section D: Biological Crystallography, 2005, 61, 1099-1106.	2.5	6
63	Hierarchical structure assembly model of rice dwarf virus particle formation. Biophysical Reviews, 2018, 10, 659-665.	1.5	5
64	An Assembly Intermediate Structure of Rice Dwarf Virus Reveals a Hierarchical Outer Capsid Shell Assembly Mechanism. Structure, 2019, 27, 439-448.e3.	1.6	5
65	Acid-stable capsid structure of Helicobacter pylori bacteriophage KHP30 by single-particle cryoelectron microscopy. Structure, 2022, 30, 300-312.e3.	1.6	5
66	High-resolution structure of phosphoketolase from Bifidobacterium longum determined by cryo-EM single-particle analysis. Journal of Structural Biology, 2022, 214, 107842.	1.3	5
67	2D hybrid analysis: Approach for building three-dimensional atomic model by electron microscopy image matching. Scientific Reports, 2017, 7, 377.	1.6	4
68	Cryo-electron tomography: moving towards revealing the viral life cycle ofRice dwarf virus. Journal of Synchrotron Radiation, 2013, 20, 826-828.	1.0	3
69	Zernike Phase Contrast Electron Microscopy: Observation of the Image Formation and Improvement of the Image Quality using Direct Detector. Microscopy and Microanalysis, 2015, 21, 2141-2142.	0.2	2
70	Fundamental Cell Morphologies Examined With Cryo-TEM of the Species in the Novel Five Genera Robustly Correlate With New Classification in Family Mycobacteriaceae. Frontiers in Microbiology, 2020, 11, 562395.	1.5	2
71	In vitro but not in planta encapsidation of Rice gall dwarf virus core particles by the outer capsid P8 protein of Rice dwarf virus expressed in transgenic rice plants. Journal of General Plant Pathology, 2006, 72, 186-189.	0.6	1
72	Outer-capsid P8 proteins of phytoreoviruses mediate secretion of assembled virus-like particles from insect cells. Journal of General Virology, 2010, 91, 2857-2861.	1.3	1

Ναούμκι Μιυαζακι

#	Article	IF	CITATIONS
73	Zernike Cryo-EM with a Direct Electron Camera Enables Tracking Protein Conformations in the Temporal Dimension. Microscopy and Microanalysis, 2015, 21, 2145-2146.	0.2	1

3P302 Observation of GFP-CL in biological specimens(27.Bioimaging,Poster,The 51st Annual Meeting of) Tj ETQq0 0.0 rgBT /Overlock 10

75	Ultimate Recovery of Low-Frequencies in Thin-film ZPC-TEM by Inverse Projector. Microscopy and Microanalysis, 2014, 20, 226-227.	0.2	0
76	Structure and Biochemical Characters of Artificial Protein Cage: Assembly and Disassembly can be Controlled. Seibutsu Butsuri, 2020, 60, 153-156.	0.0	0
77	Dynamic rotation of the protruding domain enhances the infectivity of norovirus. , 2020, 16, e1008619.		0
78	Dynamic rotation of the protruding domain enhances the infectivity of norovirus. , 2020, 16, e1008619.		0
79	Dynamic rotation of the protruding domain enhances the infectivity of norovirus. , 2020, 16, e1008619.		0